International Journal of
INTELLIGENT SYSTEMS AND APPLICATIONS IN ENGINEERING
ISSN:2147-6799 www.ijisae.org Original Research Paper

Viscous Dissipation and Joule Heating Effects on 3D Couple Stress Nanofluid Flow via Stretching Sheet

Motamari Madhu[1*, 2*], Maddileti Pasupula[3], Naveen Kumar B K[4], Aravind H R[5], R. Vijayalakshmi[6], K. Bhagya Lakshmi[7]

Submitted: 02/05/2024 **Revised**: 15/06/2024 **Accepted**: 22/06/2024

Abstract: Present work considering the heat and mass transfer on 3D ("Three Dimensional") convective motion of "couple stress" (CS) NFs ("nanofluid") with "viscous dissipation and "joule heating" effects are examined. It has many benefits in heat transfer like, apparatus chilling or vehicle thermal controlling, firewood cells, internal freezer and chiller, curative progressions etc. The flow generation has been considered at linear stretching surface (SS). Magnetic field is applied normal to the liquid motion axis and convective conditions are also encountered at the surface. The boundary layer nonlinear PDE's into ODEs by help of appropriate similarity variables. The shooting technique along with R-K-F 4th scheme is employed to the statistical solutions of resultant equations. The solutions are discussed through graphically on velocity, temperature and concentration for distinct physical parameters. Mainly finding on this work is the temperature enhances with enlarge values of heat absorption while reverse trend follows chemical reaction parameter. Moreover, the heat transfer (HT) reduction for higher values of heat absorption.

Key words: *Convective Condition; Heat and Mass Transfer; MHD; Couple Stress; Nanofluid; Non-Linear Thermal Radiation.*

Introduction

The "heat and mass transfer" (HMT) motion via SS in NFs have succeeded due to their much more important applications ("compact heat transfers, polymer technology, metallurgy, paper and glass fibre production, extrusion process, manufacturing of plastic and rubber sheets, power generators, design of nuclear reactor"). It is well known in manufacturing industries need for higher rate of HT. Present researchers concentrate the development of more rate of HT for industrial requirements. Senior researchers have reported that the influence of solid liquid mixture for HT development. Recently, HMT of Maxwell NFs motion via SS was presented Bai et al. [1]. The Micropolar liquid motion and HT in a permeable channel was explore Mirgolbabaee et al. [2]. Khan et al. [3] developed the analysis of 3D motion of Jeffrey NFs via bidirectional SS. The HMT properties of 2D EC Maxwell liquid has explored Anil Kumar and Dharmendar Reddy [4]. Khan and Azam [5] investigated the unsteady HMT mechanisms in a Marteau NFs motion via permeable SS. Almakki et al. [6] examined the unsteady 3D axisymmetric NFs via nonlinear SS. Sheikholeslami et al. [7] demonstrate analysis of HT behaviour of refrigerant NFs. Blood motion via a curved permeable artery with variable viscosity and HMT was explored by Kumawat et al. [8]. the non-Newtonian liquid motion with magnetic field and TR effects was developed [9-10].

The convection BL (boundary layer) motion via linear sheet is inordinate interest topic to the upcoming researchers. Because, in view of their much more industrial and engineering applications ("drawing of plastic films, metal and polymer extrusion, paper, metal spinning etc."). In ("additional, convective heat transfer flow has established to flow regime, energy and concentration fields around a heated stretching sheet"). There are two convection motion types like forced and free convection motion. Some of the examples include ("like electronic equipment cooled by a fan, solar receivers explored to wind current, water cooling by a forced convection, heat transfers placed in low-speed environment, water flows in the ocean and in atmosphere and many more") motion convections. The effect of NLTR on 3D non-Newtonian NFs with convective boundary was presented Mahanthesh et al. [11]. Waqas et al. [12] illustration of strategies for the enhancement of HT in NPs. Last few years, some of authors [13-18] explored the various NN NFs via various channels. Sheikholeslami et al. [19-20] developed various physical models of forced convective HT on water-Fe_3O_4-ethylen

[1]Department of Mathematics, University College, Palamuru University, Mahabubnagar-509001, Telangana, India*
[2, 3] Department of Mathematics, University College of Science and informatics, Mahatma Gandhi University, Nalgonda, Telangana, India*
[4]Assistant Professor, Department of Mechanical Engineering, M S Ramaiah Institute of Technology, Bangalore, Karnataka
[5]Assistant Professor, Department of Mathematics, Cambridge Institute of Technology, Bangalore-560036, Karnataka, India
[6]Associate Professor, Department of Mathematics, Sri Venkateswara College of Engineering (Autonomous), Karakambaadi Road, Tirupati-517507, Andrapradesh, India
[7]Assistant Professor, Department of Mathematics, Sri Venkateswara University, Tirupati-517502, Andrapradesh, India
[*]Corresponding Author: madhu.palamur@gmail.com

glycol nanomaterial. The 3D convective boundary layer NFs motion via ESS was presented Hayat et al. [21]. Díaz et al. [22] explained the mixed convection on vertical motion of finite length with a square cross section. Hayat et al. [23] explored the mixed convection motion of Sisko NFs via bidirectional SS. Ibrahim et al. [24] developed the influence of forced convection in perforation shape or geometry. Sivasankaran et al. [25] explored the mixed convection SP motion in a porous medium. Sheikholeslam and Rokni [26] explored the influence of melting free convection HT motion of NFs. Recently, some of authors [27-30] developed related and motivated work. The NPs on HT of 3D MHD NFs was presented by Zubair et al. [31].

The motivation of current study is to address the 3D couple stress Casson (CSC) NFs motion generated via SS under effects of viscous dissipation and joule heating. The HMTR produces more in motion of CSC liquid with high impact of CR via SS. The present work contributed numerical values of HMTR and comparing current work into various previous scientists' articles. We have to get good agreement.

Mathematical Formulation

The effect of NLTR on 3D MHD motion of CS NFs with chemical reaction with convective condition. The present work consideration as below:

- The SS are expressed by velocity components are $u_1 = U_w(x_1) = a_1 x_1$ and $v_1 = V_w(y_1) = b_1 y_1$ in the directions x_1 and y_1.
- The liquid motion is created by a SS at $z_1 = 0$.
- The normal magnetic field B_0 applied on the liquid direction of z_1 and perpendicular to the surface (i.e., x_1, y_1-plane). In the fluid flow occurs $z_1 > 0$ as it displays in **Figure 1**.
- The chemical reaction considering along motion direction.
- Effects of electrically conductivity, heat absorption and nonlinear thermal radiation are applied in energy direction.
- The temperature T_w is maintained on the surface.

By above conventions, formulate the mathematical equations of Cm, CM, CE and CC are shown below (see ref. **[3]**):

$$\frac{\partial u_1}{\partial x_1} + \frac{\partial v_1}{\partial y_1} + \frac{\partial w_1}{\partial z_1} = 0 \tag{1}$$

$$u_1 \frac{\partial u_1}{\partial x_1} + v_1 \frac{\partial u_1}{\partial y_1} + w_1 \frac{\partial u_1}{\partial z_1} = \upsilon \frac{\partial^2 u_1}{\partial (z_1)^2} - \upsilon' \frac{\partial^4 u_1}{\partial (z_1)^4} - \frac{\sigma_1 B_0^2}{\rho_f} u_1$$

(2)

$$u_1 \frac{\partial v_1}{\partial x_1} + v_1 \frac{\partial v_1}{\partial y_1} + w_1 \frac{\partial v_1}{\partial z_1} = \upsilon_1 \frac{\partial^2 v_1}{\partial (z_1)^2} - \upsilon' \frac{\partial^4 v_1}{\partial (z_1)^4} - \frac{\sigma_1 B_0^2}{\rho_f} v_1$$

(3)

$$\left.\begin{array}{l} u_1 \frac{\partial T_1}{\partial x_1} + v_1 \frac{\partial T_1}{\partial y_1} + w_1 \frac{\partial T_1}{\partial z_1} = \alpha^* \frac{\partial^2 T_1}{\partial (z_1)^2} - \frac{1}{(\rho_1 C_1)_f} \frac{\partial q_r}{\partial z_1} + \frac{(\rho_1 \mathrm{C}_1)_p}{(\rho_1 \mathrm{C}_1)_f} \left(D_B \left(\frac{\partial T_1}{\partial z_1} \frac{\partial T_1}{\partial z_1} \right) + \frac{D_T}{T_\infty} \left(\frac{\partial T_1}{\partial z_1} \right)^2 \right) \\ \quad + \frac{\sigma_1 B_0^2}{(\rho_1 \mathrm{C}_1)_f} (\mathrm{u}_1{}^2 + \mathrm{v}_1{}^2) + \frac{\mu_1}{(\rho_1 \mathrm{C}_1)_f} \left(\mathrm{u}_1'^2 + \mathrm{v}_1'^2 \right) - \frac{Q_0}{(\rho_1 \mathrm{C}_1)_f} (\mathrm{T}_1 - \mathrm{T}_\infty) \end{array}\right\}$$

(4)

$$u_1 \frac{\partial C_1}{\partial x_1} + v_1 \frac{\partial C_1}{\partial y_1} + w_1 \frac{\partial C_1}{\partial z_1} = D_B \left(\frac{\partial^2 C_1}{\partial (z_1)^2} \right) + \frac{D_T}{T_\infty} \left(\frac{\partial^2 T_1}{\partial (z_1)^2} \right) - K_1 (\mathrm{C}_1 - \mathrm{C}_\infty)$$

(5)

The velocity components u_1, v_1 directions of x_1 and y_1 -respectively as shown below

$$U_w(x_1) = a_1 x_1 \; V_w(y_1) = b_1 y_1$$

(6)

The relevant B.Cs. for this model as shown below

$$u_1 = a_1 x_1, \mathrm{v}_1 = b_1 y_1, \mathrm{w}_1 = 0, -k^* \frac{\partial T_1}{\partial z_1} = h_1 (\mathrm{T}_f - \mathrm{T}_1), -D^* \left(\frac{\partial C_1}{\partial z_1} \right) = h_2 \left(C_f - C_1 \right) \text{ at } \mathrm{z}_1 = 0$$
$$u_1 \to 0, \; v_1 \to 0, u_1 \to 0, v_1 \to 0, T_1 \to T_\infty, \; C_1 \to C_\infty \text{ as } z_1 \to \infty$$

(7)

According to the RA ("Roseland's Approximation") [32] non-linear radiative heat flux q_r as given by

$$q_r = -\frac{4\sigma_1}{3k^*} \frac{\partial T_1^4}{\partial z_1} = -\frac{16\sigma_1}{3k^*} T_1^3 \frac{\partial T_1}{\partial z_1}$$

(8)

Differentiate above the heat flux equation, we get

$$\frac{\partial q_r}{\partial z_1} = -\frac{16\sigma^*}{3k^*} \frac{\partial}{\partial z_1} \left(T_1^3 \frac{\partial T_1}{\partial z_1} \right)$$

(9)

Eq. (4) is transfer by utilizing above eq. (9), we have

$$
\left.\begin{aligned}
u_1\frac{\partial T_1}{\partial x_1}+v_1\frac{\partial T_1}{\partial y_1}+w_1\frac{\partial T_1}{\partial z_1}&=\alpha^*\frac{\partial^2 T_1}{\partial (z_1)^2}-\frac{1}{(\rho_1 C_1)_f}\left(\frac{16\sigma_1}{3K^*}\frac{\partial}{\partial z_1}\left(T_1^3\frac{\partial T_1}{\partial z_1}\right)\right)\\
&+\frac{(\rho_1 C_1)_p}{(\rho_1 C_1)_f}\left(D_B\left(\frac{\partial T_1}{\partial z_1}\frac{\partial T_1}{\partial z_1}\right)+\frac{D_T}{T_\infty}\left(\frac{\partial T_1}{\partial z_1}\right)^2\right)-\frac{Q_0}{(\rho_1 C_1)_f}(T_1-T_\infty)\\
&+\frac{\sigma_1 B_0^2}{(\rho_1 C_1)_f}(u_1{}^2+v_1{}^2)+\frac{\mu_1}{(\rho_1 C_1)_f}\left(u_1'^2+v_1'^2\right)
\end{aligned}\right\}
$$

(10)

The suitable similarity variables for current analysis as

$$
\left.\begin{aligned}
&u_1=a_1 x_1 f'(\eta),\quad v_1=a_1 y_1 g'(\eta),\quad w=-\sqrt{a_1\upsilon_1}\,(f(\eta)+g(\eta))\\
&\theta(\eta)=\frac{T_1-T_\infty}{T_w-T_\infty},\quad \phi(\eta)=\frac{C_1-C_\infty}{C_w-C_\infty},\quad \eta=\left(\frac{a_1}{c_1}\right)^{1/2}z_1
\end{aligned}\right\}
$$

(11)

Using the above eq. (11), translate the expressions for eq. (2)-(5) as

$$f'''=\mathrm{K}\,f^{v}+(f')^2+Mf'-f''(f+g)$$

(12)

$$g'''=\mathrm{K}\,g^{v}+(g')^2+Mg'-g''(f+g)$$

(13)

$$
\left.\begin{aligned}
&\Pr\left((f+g)\theta'-f'\theta+N_b\theta\phi'+N_t(\theta')^2\right)+M\left(Ec_x(f')^2+Ec_y(g')^2\right)\\
&\qquad=H\theta-\left(Ec_x(f'')^2+Ec_y(g'')^2\right)-\left((1+\mathrm{R}_d(1+(\theta_w-1)\theta))^3\theta'\right)'
\end{aligned}\right\}
$$

(14)

$$\phi''=-(Le\Pr(f+g)\phi'-(\mathrm{N}_t/N_b)\theta''-\gamma\phi)$$

(15)

The corresponding boundary conditions are given by

$$f=0,\quad g=0,\quad f'=1,\quad g'=\lambda,\quad \theta'=-\Gamma_1(1-\theta),\ \phi'=-\Gamma_2(1-\phi)\ \ at\ \eta=0\}$$

(16)

and

$$f'\to 0,\ g'\to 0,\ f''\to 0,\ g''\to 0,\ \theta\to 0,\ \phi\to 0,\qquad as\ \ \eta\to\infty\}$$

(17)

The skin friction coefficients, Sh_x ("Sherwood number") and Nusselt Number are follows

$$
\left.\begin{aligned}
C_{fx}&=\left(f''(0)-\mathrm{K}\,f^{iv}(0)\right)\mathrm{Re}_x^{-1/2},\\
C_{fy}&=\left(g''(0)-\mathrm{K}g^{iv}(0)\right)\mathrm{Re}_y^{-1/2},\\
Nu_x&=\left(-(1+\mathrm{R}_d\,\theta_w^3)\theta'(0)\right)\mathrm{Re}_x^{1/2},\\
\mathrm{Sh}&=-\phi'(0)\,\mathrm{Re}_x^{1/2}
\end{aligned}\right\}
$$

(18)

Results and Discussion

Figs. 2(a)-2(b) presents M on $f'(\eta)$ and $g'(\eta)$ with motion directions x_1 and y_1 respectively. It is noticed that enlarge distinct values of M in reduction along both motion directions axial and transverse velocity. Which is applicable orthogonally to the motion direction gives a resistive force is says that Lorentz force. It is very stronger resists corresponding to larger magnetic field opposes the motion of NFs useful energy is converted into heat. Moreover, the "Skin friction coefficient" reduction via x_1 and y_1 directions ($\mathrm{Re}_x^{1/2}C_{fx}, \mathrm{Re}_x^{1/2}C_{fy}$) respectively illustrated in Figs. 2(c)-2(d).

The impact of on friction motion of NFs in both $\mathrm{Re}_x^{1/2}C_{fx}$, $\mathrm{Re}_x^{1/2}C_{fy}$ illustrates respectively in **Figs. 3(a)-3(b)**. It is seen that; the "Skin friction coefficient" is low in both x_1 and y_1 directions. Physically, K is proportional to the viscosity, it makes that weaker viscous of the NFs motion in velocity field enhances with high values of K and consequently the temperature decreases.

The characteristics of λ on $f'(\eta)$, $g'(\eta)$ and $\theta(\eta)$ explored in **Figs. 4(a)-4(c)**. It is perceived that, the velocity BL ("Boundary Layer") thickness on $f'(\eta)$ along with direction-x_1 is reduction for higher statistical values of λ. While opposite trend behaviours $g'(\eta)$ along y_1 direction. Due to these figures the λ is inversely proportional to the stretching coefficient. So that, it makes high time dependent parameter decreases the stretching ratio and consequently velocity reduces at the same time temperature increases as illustrated in **Fig. 4(c)**.

Fig. 5(a) examined the H on $\theta(\eta)$. It is perceived that $\theta(\eta)$ enhances with enlarge distinct values of H. The $\theta(\eta)$ ("Temperature Profile") enhances in case of $H>0$ then it says that heat generation and related BL thickness is thinner. While the reverse trend shows in case of $H<0$ then it says that heat absorption. From Figs. 5(b)-5(c) illustrate that the H on $\mathrm{Re}_x^{-1/2}Nu_x$. It is found that the $\mathrm{Re}_x^{-1/2}Nu_x$ reduces while reverse trend shows "Mass Transfer Rate" with enlarge statistical values of H. Because, the H ("Heat Generation Parameter") is inversely proportional to weaker liquid density.

The impact of γ on $\phi(\eta)$ as explained in **Fig. 6(a)**. It is perceived that, the $\phi(\eta)$ decreases for enlarge statistical values of γ and related BL thickness is low. While opposite behaviour predict HMT as predicts in **Figs 6(b)-6(c)**. Physically, the CR is proportional to the reaction rate. Due to this it takes place without any disturbance to molecular motion of NFs is much larger. So that the concentration declines at the same time the HMT enhances.

Figs. 7(a)-7(b) discussed Γ_1 and Γ_2 on $\phi(\eta)$, respectively. It can be analysed that $\phi(\eta)$ and associated BL thickness rises with enlarge distinct statistical values of Γ_1, Γ_2 respectively. Physically, Γ_1, Γ_2 are respectively inversely proportional to the TC and MD. Due to this reason the low TC and MD on NPs liquid motion at the stretching respectively enhances HMT rate.

The investigation of R_d on $\theta(\eta)$, $\phi(\eta)$ as discussed respectively, in **Figs. 8(a)-8(b)**. It is clear that the $\theta(\eta)$, $\phi(\eta)$ enhancement for large distinct statistical values of R_d. Physically, the TR is inversely proportional to the product of heat capacity and liquid density. So that, the liquid NFs rise more heat from the SS for enlarge values of R_d and related thermal BL thickness enhances, consequently the concentration field also enhances.

Figs. 9(a)-9(b) predicts that the θ_w on $\theta(\eta)$, $\phi(\eta)$ respectively. It is noticed that θ_w with enlarged statistical values of $\theta(\eta)$. Physically, the θ_w is ratio between convective surface temperature and uniform ambient temperature. The motion NPs increase heat from the surface for higher values of θ_w. So that, the temperature increases and consequently concentration is high and associated BL thickness is thinner.

Fig. 10 illustrate that the characteristics of Le on $\phi(\eta)$. It is clear that $\phi(\eta)$ enhances with large values of Le and related concentration BL thickness is thinner. Physically, the Le ("Lewis Number") is inversely proportional to the Brownian diffusion coefficient. The weaker Brownian diffusion coefficient for enlarge statistical values of Le and it is creating more concentration.

The influence of Ec_x, Ec_y on $\theta(\eta)$ as demonstrates in Figs. **11(a)-11(b)**. It is observed that, the $\theta(\eta)$ increases along with x_1, y_1 -directions for distinct statistical values of Ec_{x_1}, Ec_{y_1} respectively. It is fact that, the reason is "Eckert number" has reaction between the surface temperature and ambient temperature also viscous dissipation effect on NFs particles. Moreover, the heat capacity involved in this case because which is inversely proportional to the "Eckert number".

Table. 1 explore that, the numerical values of HTR in various physical parameters for $\lambda = 0$ and **Table 2, Table 3** shown MTR in different physical parameters for $\lambda = 0$, $\Gamma_1 = 0 = \Gamma_2$ and $\Gamma_1 = 0.5 = \Gamma_2$ respectively . The statistical results of horizontal and normal velocity gradients of a CSC liquid. The finding results are matched with those of Wang **[33]**, Ariel **[34]** and Ghosh et al. **[35]** for specific cases (i.e., $M = 0$, $K = 0$) as predicted in **Table. 4**. It is detected that the upshots are in very good agreement up to six decimal places.

Conclusion

The current work as a statistical model for the convective HMT in 3D MHD CS NFs ("nanofluid") motion with NLTR and chemical reaction. From this investigation, we have mainly noticed unique results as below:

- The $\mathrm{Re}_x^{-1/2} Nu_x$ decreases of heat generation/absorption parameter while opposite trend follows $\mathrm{Sh}\mathrm{Re}_x^{-1/2}$ profile with distinct choosing values of H.
- The HMT field's enhancement of chemical reaction parameter.
- Nanoparticle concentration enhances of temperature Biot number and concentration Biot number respectively.
- The temperature and concentration profile increases of TR parameter as well as temperature parameter enhances.
- The temperature field increases of Brownian motion parameter while reverse trend behaviour shows thermophoresis parameter.
- The NPs concentration declines of thermophoresis parameter.

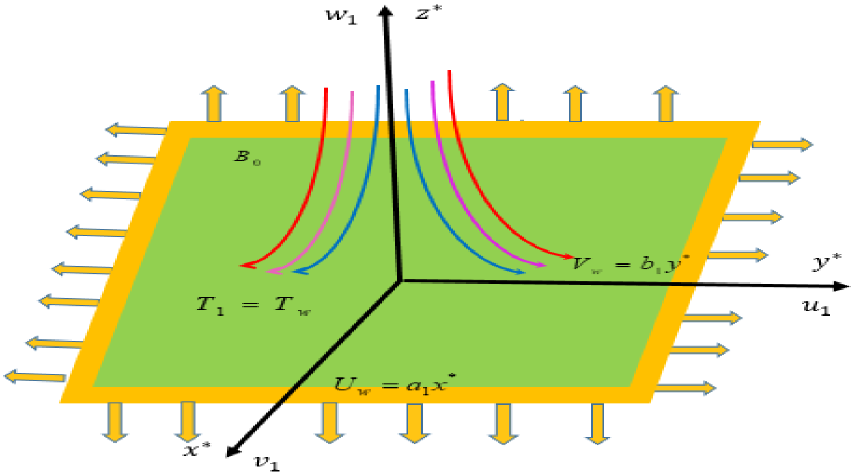

Fig 1: Physical model of the problem

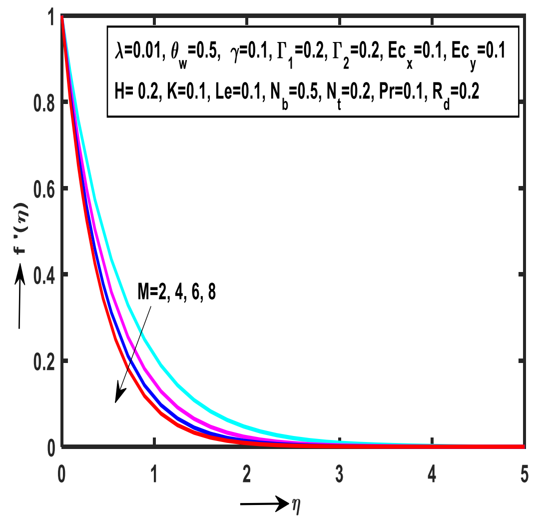

Fig 2(a): Impact of M on $f'(\eta)$

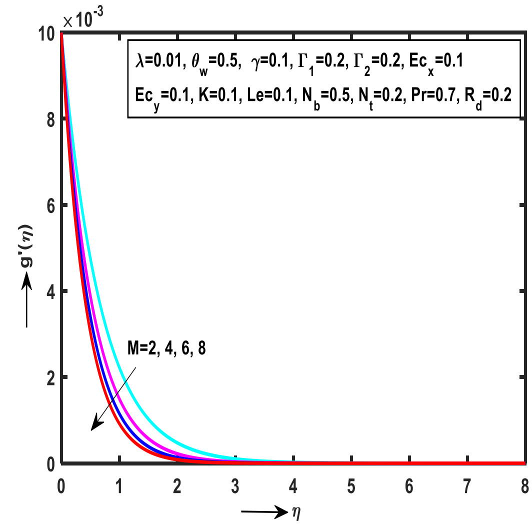

Fig 2(b): Impact of M on $g'(\eta)$

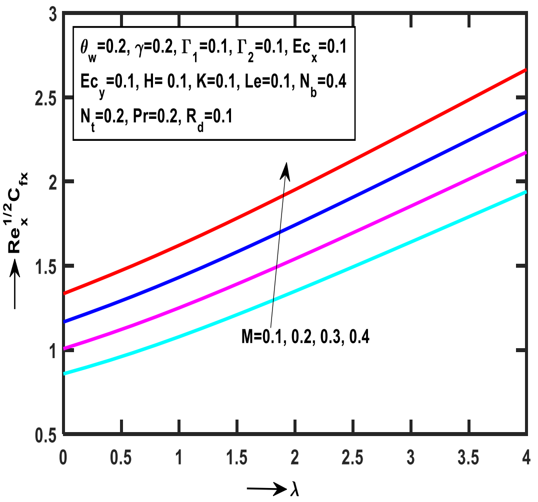

Fig 2(c): Impact of M on $\mathrm{Re}_x^{1/2} C_{fx}$

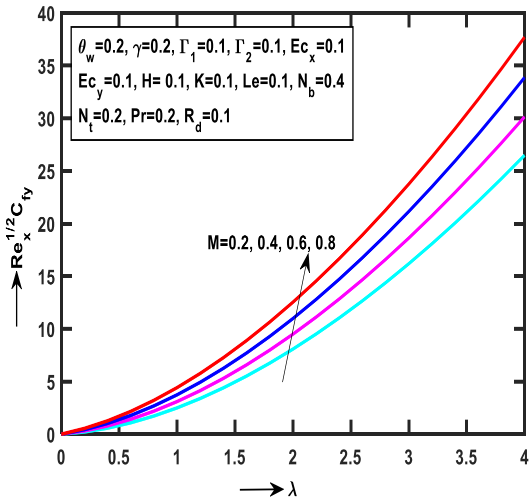

Fig 2(d): Impact of M on $\mathrm{Re}_x^{1/2} C_{fy}$

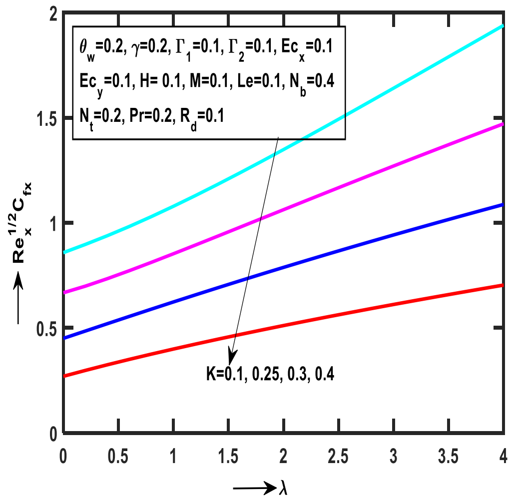

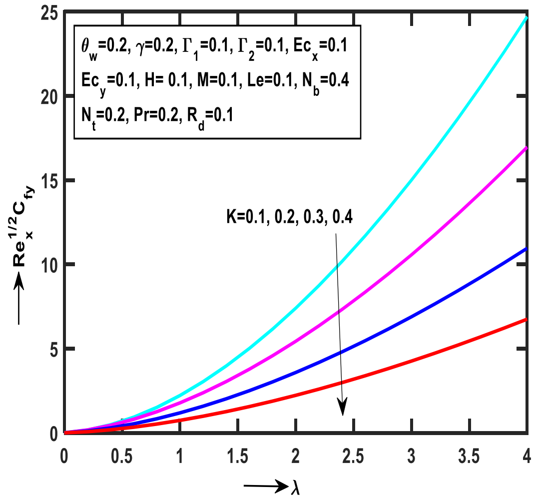

Fig 3(a): Impact of K on $\mathrm{Re}_x^{1/2} C_{fx}$ **Fig 3(b):** Impacct of K on $\mathrm{Re}_x^{-1/2} C_{fy}$

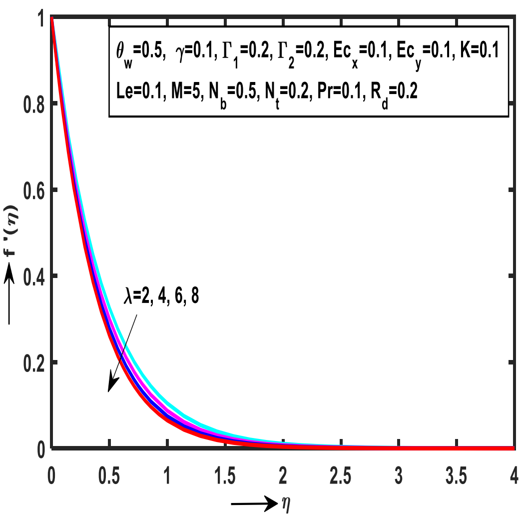

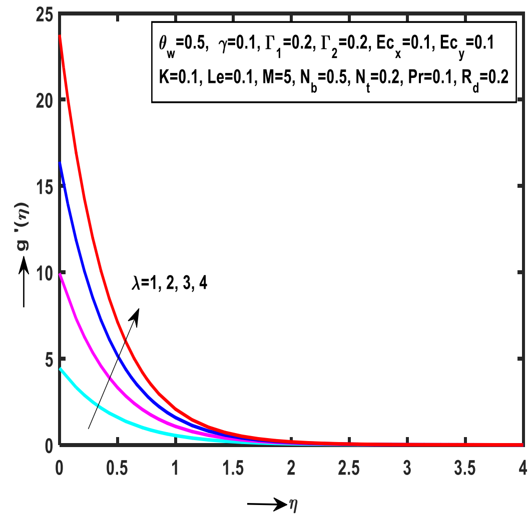

Fig 4(a): Impact of λ on $f'(\eta)$ **Fig 4(b):** Impact of λ on $g'(\eta)$

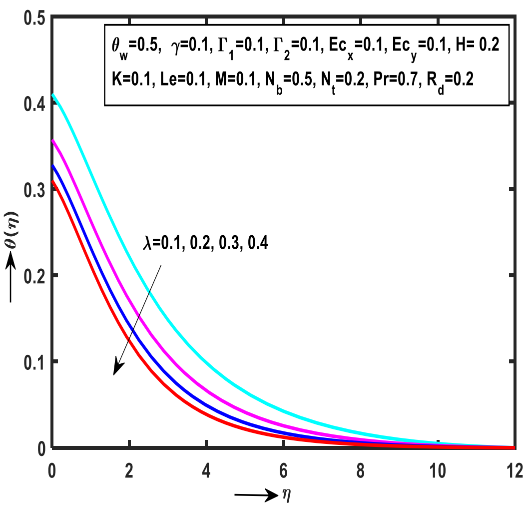

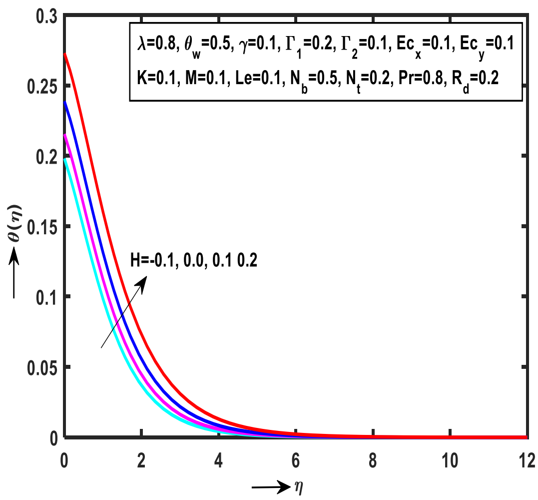

Fig 4(c): Impact of λ on $\theta(\eta)$ **Fig 5(a):** Impact of H on $\theta(\eta)$

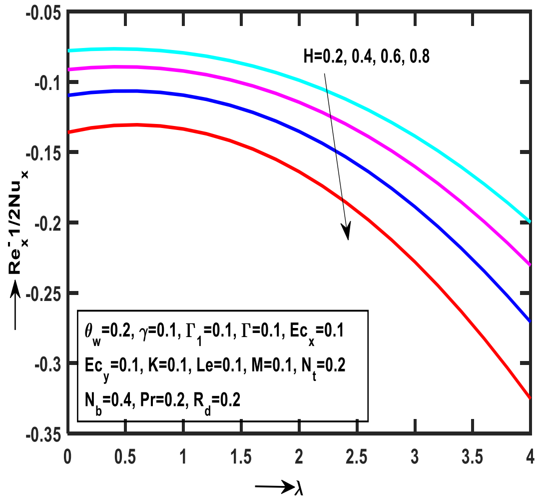

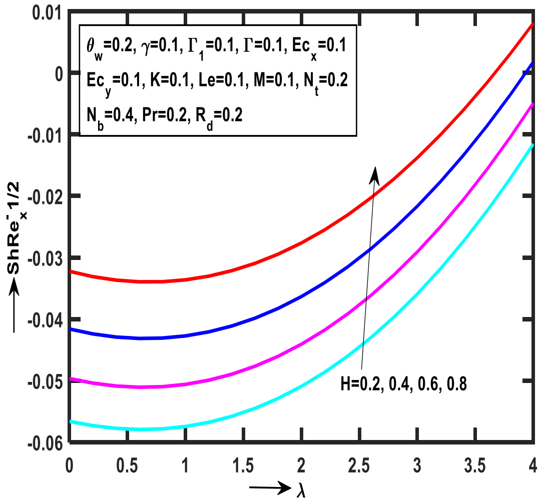

Fig 5(b): Impact of H on $\mathrm{Re}_x^{-1/2} Nu_x$ **Fig 5(c):** Impact of H on $\mathrm{Sh}\,\mathrm{Re}_x^{-1/2}$

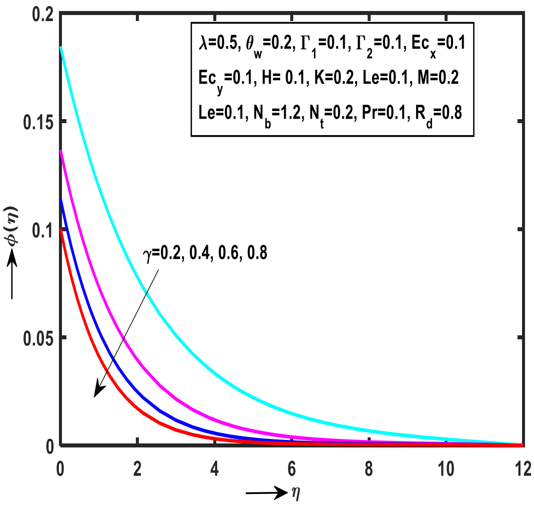

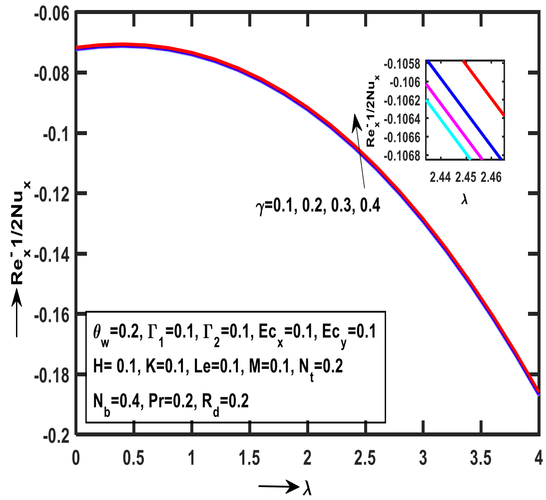

Fig 6(a): Impact of γ on $\theta(\eta)$ **Fig 6(b):** Impact of γ on $\mathrm{Re}_x^{-1/2} Nu_x$

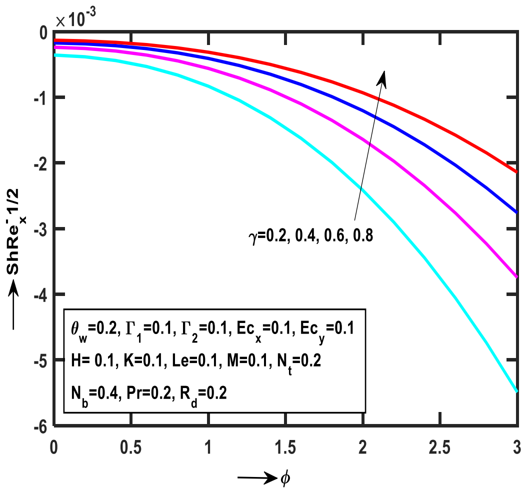

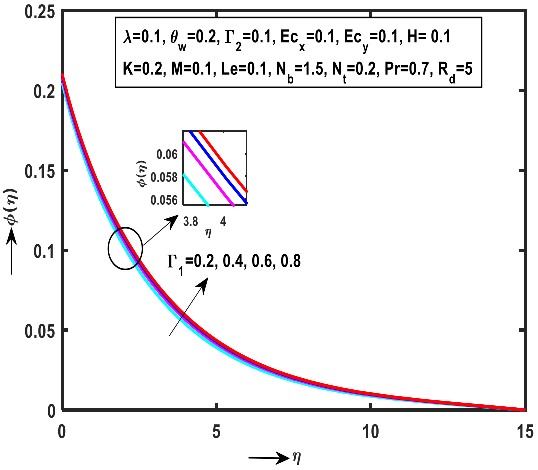

Fig 6(c): Impact of γ on $\mathrm{Sh}\,\mathrm{Re}_x^{-1/2}$ **Fig 7(a):** Impact of Γ_1 on $\phi(\eta)$

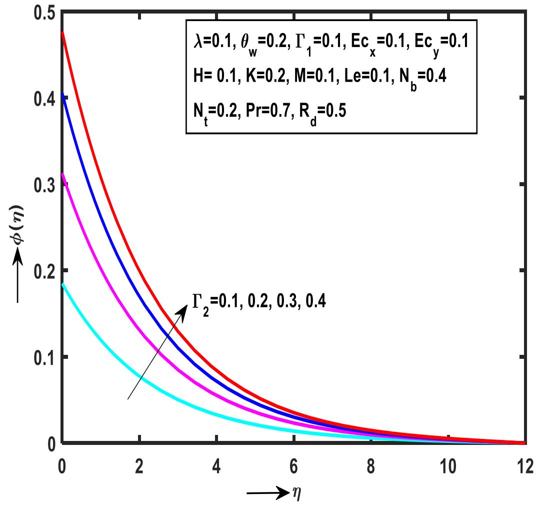

Fig 7(b): Impact of Γ_2 on $\phi(\eta)$

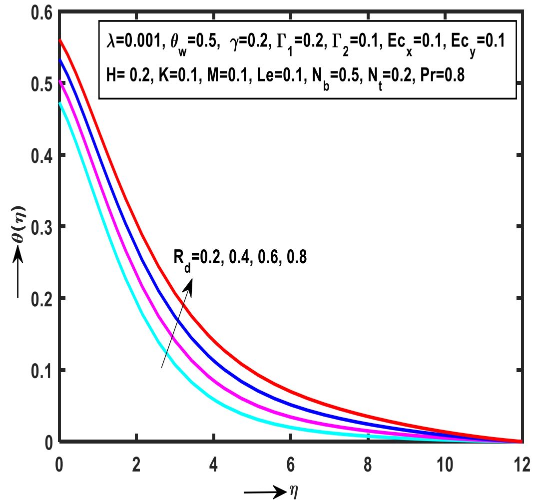

Fig 8(a): Impact of R_d on $\theta(\eta)$

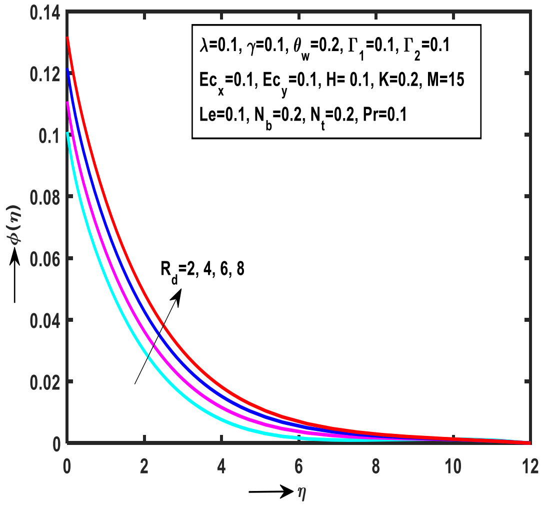

Fig 8(b): Impact of R_d on $\phi(\eta)$

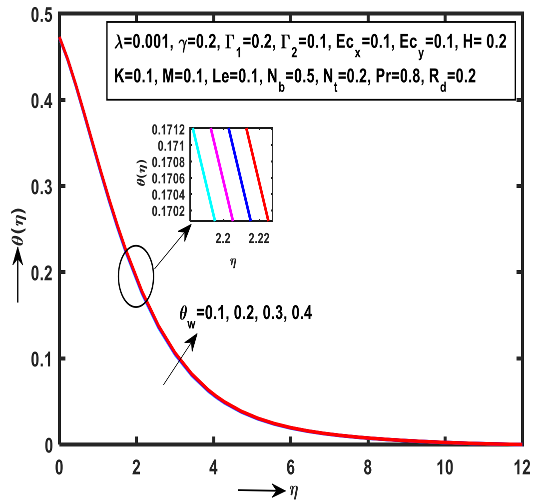

Fig 9(a): Impact of θ_w on $\theta(\eta)$

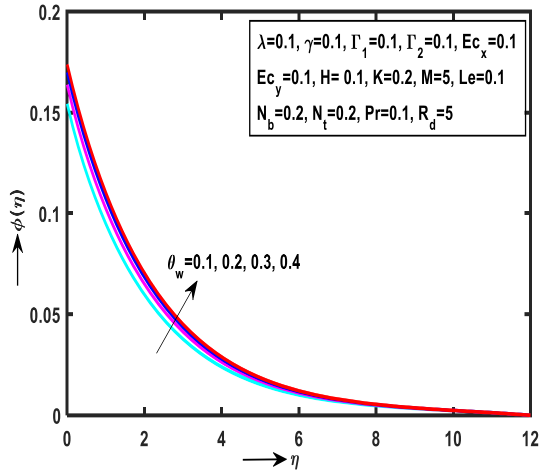

Fig 9(b): Impact of θ_w on $\phi(\eta)$

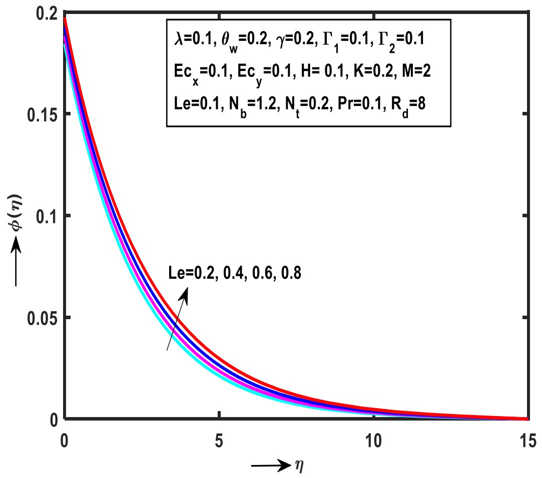

Fig 10: Impact of Le on $\phi(\eta)$

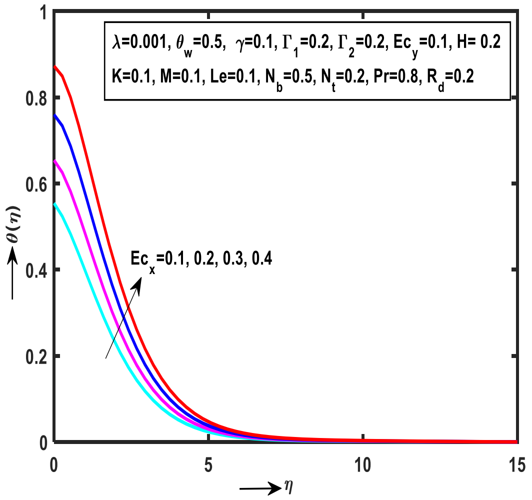

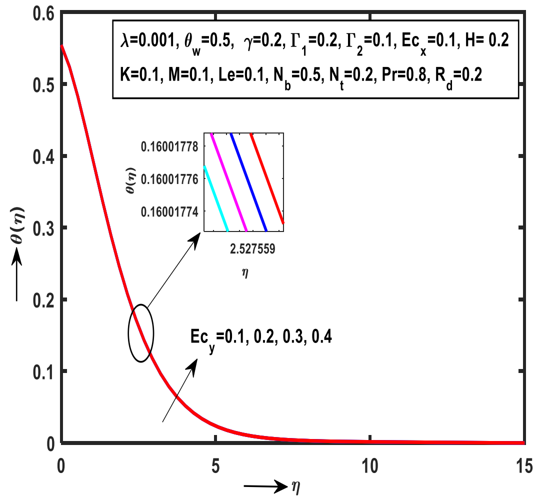

Fig 11(a): Impact of Ec_x on $\theta(\eta)$ **Fig 11(b):** Impact of Ec_y on $\theta(\eta)$

Table 1: Numerical values of $\mathrm{Re}_x^{-1/2} Nu_x$ with different parameters of K, Le, $\Pr$, R_d, M, N_t, N_b, θ_w, H, Γ_1, Γ_2, γ, Ec_x, and Ec_y for $\lambda = 0$.

K	Le	$\Pr$	R_d	M	N_t	N_b	θ_w	H	Γ_1	Γ_2	γ	Ec_x	Ec_y	$\mathrm{Re}_x^{-1/2} Nu_x$
0.2														-0.07246
0.4														-0.06952
0.6														-0.06825
0.8														-0.06751
	0.1													-0.07156
	0.2													-0.07241
	0.3													-0.07235
	0.4													-0.07227
		0.1												-0.06447
		0.2												-0.07246
		0.3												-0.07809
		0.4												-0.08204
			0.2											-0.07146
			0.4											-0.07111
			0.6											-0.07064
			0.8											-0.07011
				0.2										-0.07867
				0.4										-0.08429
				0.6										-0.08984
				0.8										-0.09532
					0.1									-0.07123
					0.2									-0.07146
					0.3									-0.07164
					0.4									-0.07167
						0.2								-0.07209
						0.4								-0.07146
						0.6								-0.07072
						0.8								-0.06998
							0.1							-0.00753
							0.2							-0.07251
							0.3							-0.07249

0.4							-0.07248
	0.2						-0.07787
	0.4						-0.09130
	0.6						-0.10960
	0.8						-0.13590
		0.1					-0.07244
		0.2					-0.15430
		0.3					-0.23040
		0.4					-0.29700
			0.1				-0.07160
			0.2				-0.07065
			0.3				-0.07005
			0.4				-0.06964
				0.1			-0.07230
				0.2			-0.07146
				0.3			-0.07125
				0.4			-0.07088
					0.2		-0.83540
					0.4		-0.10880
					0.6		-0.13810
					0.8		-0.17140
						0.1	-0.07230
						0.2	-0.09919
						0.3	-0.12720
						0.4	-0.15590

Table 2: Numerical values of $\mathrm{Re}_x^{-1/2}\mathrm{Sh}$ with different parameters of K, $\Pr$, R_d, M, θ_w, H, Γ_1, Γ_2, γ, Ec_x, *and* Ec_y for $\lambda = 0$.

K	$\Pr$	R_d	M	θ_w	H	Γ_1	Γ_2	γ	Ec_x	Ec_y	$\mathrm{Re}_x^{-1/2} Sh$
0.2											-0.14360
0.4											-0.15370
0.6											-0.16000
0.8											-0.16450
	0.1										-0.18330
	0.2										-0.21630
	0.3										-0.28130
	0.4										-0.40730
		0.2									-0.21630
		0.4									-0.21350
		0.6									-0.21160
		0.8									-0.21050
			0.2								-0.13150
			0.4								-0.12290
			0.6								-0.11480
			0.8								-0.10710
				0.1							-0.21890
				0.2							-0.21630
				0.3							-0.21660
				0.4							-0.21710
					0.2						-0.05662
					0.4						-0.04966
					0.6						-0.04161
					0.8						-0.03224

0.1					-0.14360
0.2					-0.16260
0.3					-0.17650
0.4					-0.18720
	0.1				-0.14360
	0.2				-0.31320
	0.3				-0.43390
	0.4				-0.52040
		0.2			-0.00035
		0.4			-0.00017
		0.6			-0.00018
		0.8			-0.00014
			0.2		-0.05372
			0.4		-0.04241
			0.6		-0.03217
			0.8		-0.02309
				0.1	-0.31450
				0.2	-0.22660
				0.3	-0.13540
				0.4	-0.04279

Table 3: Numerical values of $\mathrm{Re}_x^{-1/2}\mathrm{Sh}$ with different parameters of K, $\Pr$, R_d, M, θ_w, H, γ, Ec_x, *and* Ec_y for $\lambda = 0$.

K	$\Pr$	R_d	M	θ_w	H	Ec_x	Ec_y	$\mathrm{Re}_x^{-1/2}\mathrm{Sh}$	
								$\Gamma_1 = 0 = \Gamma_2$	$\Gamma_1 = 0.5 = \Gamma_2$
0.2								-0.004583	-0.62410
0.4								-0.003899	-0.63660
0.6								-0.003763	-0.64450
0.8								-0.003520	-0.65010
	0.1							-0.000188	-0.57410
	0.2							-0.000712	-0.61500
	0.3							-0.001507	-0.66420
	0.4							-0.002517	-0.72230
		0.2						-0.005096	-0.61500
		0.4						-0.003605	-0.61080
		0.6						-0.003899	-0.60740
		0.8						-0.003064	-0.60450
			0.2					-0.006046	-0.61000
			0.4					-0.008054	-0.60060
			0.6					-0.010190	-0.59170
			0.8					-0.012450	-0.58340
				0.1				-0.005096	-0.26490
				0.2				-0.005454	-0.26500
				0.3				-0.005411	-0.26520
				0.4				-0.005367	-0.26530
					0.2			-0.006056	-0.59670
					0.4			-0.009140	-0.55460
					0.6			-0.015870	-0.50300
					0.8			-0.003723	-0.43770
						0.1		-0.011890	-0.60230
						0.2		-0.030940	-0.57720
						0.3		-0.057920	-0.55250
						0.4		-0.093500	-0.52820

			0.2	-0.001375	-0.39870
			0.4	-0.002809	-0.33220
			0.6	-0.004307	-0.26500
0.8	-0.007827	-0.19770			

Table. 4 Comparison of $-f''(0)$ and $-g''(0)$ at the sheet in x_1 and y_1 directions of ordinary fluid in the absence of ($K=0$ and $M=0$).

λ	**Wang** [33] $-f''(0)$	**Ariel (Exact solution)** [34] $-f''(0)$	**Ghosh** [35] $-f''(0)$	**Present study** $-f''(0)$	**Wang** [33] $-g''(0)$	**Ariel (Exact solution)** [34] $-g''(0)$	**Ghosh** [35] $-g''(0)$	**Present study** $-g''(0)$
0.00	1.0000	1.0000		1.00000	0.0000			0.00000
0.10				1.02026				0.06684
0.20		1.0394	1.0395	1.03949		0.1487	1.14874	0.148737
0.25	1.0488			1.04881	0.1945			0.194564
0.30				1.05795				0.243361
0.40		1.0757	1.0757	1.07578		0.3492	1.34921	0.349210
0.50	1.0930			1.09309	0.4652			0.465206
0.60		1.1099	1.1099	1.10994		0.5905	1.59053	0.590530
0.70				1.12639				0.724533
0.75	1.1344			1.13448	0.7946			0.794627
0.80		1.1424	1.1424	1.14248		0.8666	0.86668	0.866684
0.90				1.15825				1.016539
1.00	1.1737	1.1737	1.1737	1.17372	1.1737	0.1737	1.17372	1.173721

References

[1] Y. Bai, X. Liu, Y. Zhang, and M. Zhang, "Stagnation-point heat and mass transfer of MHD Maxwell nanofluids over a stretching surface in the presence of thermophoresis," *J. Mol. Liq.*, vol. 224, pp. 1172–1180, Dec 2016. DOI: 10.1016/J.M OLLI Q.201 6.10 .082.

[2] H. Mirgolbabaee, S.T. Ledari, and D.D. Ganji, "Semi - analytical investigation on micropolar fluid flow and heat transfer in a permeable channel using AGM," *J. Assoc. Arab Univ. Basic Appl. Sci.*, vol. 24, no. 1, pp. 213–222, Feb 2017. DOI: 10.1016/J.JA UBAS.2017.01.002.

[3] M.I. Khan, A. Alsaedi, S.A. Shehzad, and T. Hayat, "Hydromagnetic nonlinear thermally radiative nanoliquid flow with Newtonian heat and mass conditions," *Results Phys*., vol. 7, pp. 2255–2260, Jul 2017. DOI: 10.1016/J.RINP.2017.06.035.

[4] M. Anil Kumar and Y. Dharmendar Reddy, "Thermal radiation and chemical reaction influence on MHD boundary layer flow of a Maxwell fluid over a stretching sheet containing nanoparticles," *J. Therm. Anal. Calorim*., vol. 148, pp. 6301–6309, Jul 2023. DOI: 10.1007/s10973-023-12097-1.

[5] M. Khan and M. Azam, "Unsteady heat and mass transfer mechanisms in MHD Carreau nanofluid flow," *J. Mol. Liq*., vol. 225, pp. 554–562, Jan 2017. DOI: 10.1016/J.MOLL IQ .2 016.11.107.

[6] M. Almakki, S. Dey, S. Mondal, and P. Sibanda, "On unsteady three-dimensional axisymmetric MHD nanofluid flow with entropy generation and thermo-diffusion effects on a non-linear stretching sheet," *Entropy.*, vol. 19, no. 7, Jul 2017. DOI: 10.3390/E1907016 8.

[7] M. Sheikholeslami, M. Darzi, and M.K. Sadoughi, "Heat transfer improvement and pressure drop during condensation of refrigerant-based nanofluid; an experimental procedure," *Int. J. Heat Mass Transf*., vol. 122, pp. 643-650, Jul 2018. DOI: 10.1016 /J.IJH EATMASSTRANSFER.2018.02.015.

[8] C. Kumawat, B.K. Sharma, Q.M. Al-Mdallal, and M. Rahimi-Gorji, "Entropy generation for MHD two phase blood flow through a curved permeable artery having variable vis cosity with heat and mass transfer," *Int. Comm. Heat Mass Transf.*, vol. 133, no. 20, Mar 2022. DOI: 10.1016/j.icheatmasstransfer.2022.105954.

[9] P.B.A. Reddy, S. Jakeer, H.T. Basha, S.R.R. Reddy, and T.M. Kumar, "Multi-layer artificial neural

network modeling of entropy generation on MHD stagnation point flow of Cross-nanofluid," *Waves Random Complex Media*., pp. 1–28, Apr 2022. DOI: 1 0.1080/17455030.2022.2067375.

[10] H.T. Basha, S.R.R. Reddy, V. Ramachandra Prasad K. Joong Son, N. Ameer Ahmmad, and N. Akkurt, "Non-similar solutions and sensitivity analysis of nano-magnetic Eyring - Powell fluid flow over a circular cylinder with nonlinear convection," *Waves Random Complex Media.*, pp. 1-39, Oct 2022. DOI: 10.1080/17455030.2022.2128466.

[11] B. Mahanthesh, B.J. Gireesha, G.T. Thammanna, S.A. Shehzad, F.M. Abbasi, and R.S.R. Gorla, "Nonlinear convection in nano Maxwell fluid with nonlinear thermal radiation: A three-dimensional study," *Alexandria Eng.* J., vol. 57, no. 3, pp. 1927 - 1935, Sep 2 018. DOI: 10.1016/J.AEJ.2017.03.037.

[12] H. Waqas, U. Farooq, D. Liu, M. Abid, M. Imran, and M. Taseer, "Heat transfer analysis of hybrid nanofluid flow with thermal radiation through a stretching sheet: A comparative study," *Int. Comm. Heat Mass Transf., vol.* 138, Nov 2022. DOI: 10.1016/j.icheatmasstransfer .2022.106303.

[13] K.U. Rehman, A. Qaiser, M.Y. Malik, and U. Ali, "Numerical communication for MHD thermally stratified dual convection flow of Casson fluid yields by stretching cylinder," *Chinese J. Phys.*, vol. 55, no. 4, pp. 1605–1614, Aug 2017. DOI: 10.10 16/J.CJPH.2017.05.002.

[14] W. Ibrahim, "Nonlinear radiative heat transfer in magnetohydrodynamic (MHD) stagnation point flow of nanofluid past a stretching sheet with convective boundary condition," *Propulsion. Power Res*., vol. 4, no. 4, pp. 230–239, Dec 2015. DOI: 10.1016/J.JPPR .2015.07.007.

[15] I.V. Miroshnichenko, M.A. Sheremet, I. Pop, and A. Ishak, "Convective heat transfer of micropolar fluid in a horizontal wavy channel under the local heating," *Int. J. Mech. Sci.,* vol. 128–129, pp. 541–549, Aug 2017. DOI: 10.1016/J.IJMECSCI.2017.05.013.

[16] S.R.R. Reddy, "Entropy generation on biomagnetic gold-copper/blood hybrid nanofluid flow driven by electrokinetic force in a horizontal irregular channel with bioconvection phenomenon," *Proc. Inst. Mech. Eng. Part C J. Mech. Eng. Sci*., vol. 237, no. 7, pp. 1–16, Oct 2022. DOI: 10.1177/09544062221130018.

[17] S.R.R. Reddy, C.S.K. Raju, S.R. Gunakala, H.T. Basha, and S.J. Yook, "Bio-magnetic pulsatile CuO−Fe3O4 hybrid nanofluid flow in a vertical irregular channel in a suspension of body acceleration," *Int. Comm. Heat Mass Transf.*, vol. 135, Jun 2022. DOI: 10.1016/J.ICHEATMASSTRANSFER.2022.106151 .

[18] S.R.R. Reddy, "Bio-magnetic pulsatile flow of Ti-alloy-Au/blood couple stress hybrid nanofluid in a rotating channel," *Waves Random Complex Media*., pp. 1-24, Nov 2022. DOI: 10.1080/17455030.2022.2150333.

[19] M. Sheikholeslami, T. Hayat, A. Alsaedi, and S. Abelman, "Numerical analysis of EHD na nofluid force convective heat transfer considering electric field dependent viscosity," *Int. J. Heat Mass Transf.*, vol. 108, pp. 2558–2565, May 2017. DOI: 10. 101J.HEAMA SSTRANSFER.2016.10.099.

[20] M. Sheikholeslami, M.B. Gerdroodbary, and D.D. Ganji, "Numerical investigation of forced convective heat transfer of Fe3O4-water nanofluid in the presence of external magnetic source," *Comp. Methods Appl. Mech. Eng.*, vol. 315, pp. 831-845, Mar 2017. DOI: 10.1016/J.CMA.2016.11.021.

[21] T. Hayat, I. Ullah, T. Muhammad, and A. Alsaedi, "Magnetohydrodynamic (MHD) three-dimensional flow of second grade nanofluid by a convectively heated exponentially stretching surface," *J. Mol. Liq.*, vol. 220, pp. 1004–1012, Aug 2016. DOI: 10.1016/J. MOLLIQ.2016.05.024.

[22] K. Ortiz-Díaz, F. Oviedo-Tolentino, R. Romero-Méndez, F.G. Pérez-Gutiérrez, and L.A. M artínez-Suástegui, "Effect of light penetration depth during laminar mixed convection in a discretely, asymmetrically and volumetrically laser-heated vertical channel of finite length," *Exp. Therm. Fluid Sci.*, vol. 86, pp. 117-129, Sep 2017. DOI: 10.1016/J.EXP TH ERM F LUSCI.2017.03.027.

[23] T. Hayat, I. Ullah, A. Alsaedi, M. Waqas, and B. Ahmad, "Three-dimensional mixed convection flow of Sisko nanoliquid," *Int. J. Mech. Sci*., vol. 133, pp. 273–282, Nov 2017. DOI: 10.1016/J.IJMECSCI.2017.07.037.

[24] T.K. Ibrahim, *et al*. "Experimental study on the effect of perforations shapes on vertical heated fins performance under forced convection heat transfer," *Int. J. Heat Mass Transf.*, vol. 118, Mar 2018, pp. 832–846. DOI: 10.1016/J.IJHEATM ASSTRANSFER.2017.11.047.

[25] S. Sivasankaran, H. Niranjan, and M. Bhuvaneswari, "Chemical reaction, radiation and slip effects on MHD mixed convection stagnation-point flow in a porous medium with convective boundary condition," *Int. J. Num. Methods Heat Fluid Flow*., Vol. 27, no. 2, pp. 454 -470, Feb 2017. DOI: 10.1108/HFF-02-2016-0044.

[26] M. Sheikholeslami, and H.B. Rokni, "Melting heat transfer influence on nanofluid flow inside a cavity in existence of magnetic field," *Int. J. Heat Mass Transf.*, vol. 114, pp. 517–526, Nov 2017. DOI: 10.1016/ J. IJHEATMASSTRANSFER.2017.06.0 92.

[27] F. Wang, N. Tarakaramu, N. Sivakumar, P.V. Satya Narayana, D. Harish Babu, and R. Sivajothi, “Three dimensional nanofluid motion with convective boundary condition in presents of nonlinear thermal radiation via stretching sheet," *J. Indian Chem. Soc*., vol. 100, no.2, Feb 2023. DOI: 10.1016/j.jics.2023.100887.

[28] F. Wang, N. Tarakaramu, M.V. Govindaraju, N. Sivakumar, K. Bhagya Lakshmi, P.V. Satya Narayana, and R. Sivajothi, “Activation energy on three-dimensional Casson nano fluid motion via stretching sheet: Implementation of Buongiorno’s model,” *J. Indian Chem. Soc*., vol. 100, no. 2, Feb 2023. DOI: 10.1016/j.jics.2023.10 0886.

[29] N. Tarakaramu, P.V. Satya Narayana, N. Sivakumar, D. Harish Babu, and K. Bhagya Lakshmi, "Convective conditions on 3D magnetohydrodynamic (MHD) non-Newtonian nanofluid flow with nonlinear thermal radiation and heat absorption: a numerical analysis," *J. Nanofluids.*, vol. 12, No. 2, pp. 448-457, Mar 2023. DOI: 10.1166/jon. 2023.1939.

[30] S. Jagadeesh, M. Chenna Krishna Reddy, N. Tarakaramu, N. Sivakumar, and R. Sivajothi, "Nonlinear Thermal Radiation Effect on 3D Nanofluid Flow with Convective and Slip Condition via Stretching/Shrinking Surface," *Int. J. Appl. Comput. Math*., Sep 2022. DOI: 10.21203/ rs.3.rs - 2057507 /v1.

[31] T. Zubair, *et al*. "Investigation of shape effects of Cu-nanoparticle on heat transfer of MHD rotating flow over nonlinear stretching sheet," *Alex. Eng. J.,* vol. 61, no. 6, pp. 4457-4466, Jun 2022. DOI: 10.1016/j.aej.2021.10.007

[32] M. Q. Brewster, Thermal Radiative Transfer Properties, *New York*, *Wiley,* 1972.

[33] C.Y. Wang, "The three-dimensional flow due to a stretching flat surface," *Phys. Fluids.*, vol. 27, no. 8, pp. 1915- 1917, Aug 1984. DOI: 10.1063/1.864868.

[34] P.D. Ariel, "The three-dimensional flow past a stretching sheet and the Homotopy perturbation method," *Comp. Math. with Appl.*, vol. 54, nos. 7-8, pp. 920 -925, Oct 2007. DOI: 10.10 16/J.CAMWA.2006.12.066.

[35] S. Ghosh, S. Mukhopadhyay, and T. Hayat, "Couple stress effects on three-dimensional flow of magnetite-water based nanofluid over an extended surface in presence of non-linear thermal radiation," *Int. J. Appl. Comp. Math*., vol. 4, no. 11, pp. 1-18, 2018. DOI: 10. 1007/S40819-017-0443-0/METRICS.

Nomenclature	
a_1, b_1 Constants	T_w Constant fluid Temperature of the wall
u_1, v_1, w_1 velocity components along $x_1,\ y_1, z_1$	T_∞ Fluid temperature far away from the surface
C_f Skin friction coefficient	U_w Stretching velocity
C_w Variable concentration	***Greek symbols***
C_∞ Uniform ambient concentration	μ_1 Dynamic viscosity
D_B Brownian diffusion	$\alpha^* = \dfrac{k_f}{(\rho_1 C_1)_f}$ Thermal diffusivity
D_T Thermophoresis diffusion	η Similarity variable
$Ec_x = \dfrac{u_w^2}{C_f(T_w - T_\infty)}$ Eckert number in the direction of x_1	ϕ Dimensionless concentration
$Ec_y = \dfrac{v_w^2}{C_f(T_w - T_\infty)}$ Eckert number in direction of y_1	$\lambda = \dfrac{b_1}{a_1}$ Ratio parameter
f Dimensionless stream function	$\Gamma_2 = \dfrac{h_2}{D}\sqrt{\dfrac{a_1}{\upsilon_1}}$ Concentration Biot number

f' Dimensionless velocity	$\Gamma_1 = \frac{h_1}{k}\sqrt{\frac{a_1}{\upsilon_1}}$ Temperation Biot number
$K = \frac{a_1 \upsilon'}{\upsilon_1^2}$ Couple Stress Parameter	$\upsilon_1 = \frac{\mu_1}{\rho_f}$ Kinematic viscosity
k^* Mean absorption coefficient	σ_1 Boltzmann constant
$Le = \frac{\alpha^*}{D_B}$ Lewis number	θ Dimensionless temperature
$M = \frac{\sigma_1 B_0^2}{a_1 \rho_f}$ magnetic field parameter	$\upsilon' = \frac{n}{\rho_f}$ Couple stress viscosity
$N_t = \frac{D_T(\rho_1 C_1)_p}{T_\infty(\rho_1 C_1)_f}(T_w - T_\infty)$ Thermophoresis parameter	$(\rho c_p)_f$ Heat capacity of the field
$N_b = \frac{D_B(\rho_1 C_1)_p}{\upsilon_1(\rho_1 C_1)_f}(C_w - C_\infty)$ Brownian motion coefficient	$(\rho c_p)_p$ Heat capacity of the nanoparticle material
Nu_x Nusselt number	ρ_f Fluid density
$\Pr = \left(\frac{\upsilon_1}{\alpha^*}\right)$ Prandtl number	ρ_1 Fluid density
q_r radiative heat flux	k Thermal conductivity (m^2/s)
$R_d = \frac{16\sigma_1 T_\infty^3}{3kK^*}$ radiation parameter	D Mass diffusivity
Re_x Reynolds number	***Subscripts***
T_1 Fluid Temperature	w wall mass transfer velocity
Abbreviations	
CS Couple Stress	ODE Ordinary Differential Equations
NFs Nanofluids	HT Heat Transfer
SS Stretching Sheet	MHD Magnetohydrodynamic
ESS Exponential Stretching Sheet	NLTR Nonlinear Thermal Radiation
PDE Partial Differential Equations	HMT Heat and Mass Transfer
NN Nonnewtonian	NPs Nanoparticles
CSE Couple Stress Casson	MD Mass Diffusivity
TC Thermal Conductivity	TR Thermal Radiation
CR Chemical Reaction	